Harmonic Generation from Relativistic Plasma Surfaces in Ultrasteep Plasma Density Gradients

C. Rödel,[1,2] D. an der Brügge,[3] J. Bierbach,[1] M. Yeung,[4] T. Hahn,[5] B. Dromey,[4] S. Herzer,[1] S. Fuchs,[1] A. Galestian Pour,[1]
E. Eckner,[1] M. Behmke,[5] M. Cerchez,[5] O. Jäckel,[1,2] D. Hemmers,[5] T. Toncian,[5] M. C. Kaluza,[1,2] A. Belyanin,[6]
G. Pretzler,[5] O. Willi,[5] A. Pukhov,[3] M. Zepf,[4,2] and G. G. Paulus[1,2]

[1]*Institut für Optik und Quantenelektronik, Friedrich-Schiller-Universität, Max-Wien-Platz 1, 07743 Jena, Germany*
[2]*Helmholtz Institut, Fröbelstieg 13, 07743 Jena, Germany*
[3]*Institut für Theoretische Physik, Heinrich-Heine Universität, Universitätsstraße 1, 40225 Düsseldorf, Germany*
[4]*Centre for Plasma Physics, School of Mathematics and Physics, Queen's University Belfast, BT7 1NN, United Kingdom*
[5]*Institut für Laser-und Plasmaphysik, Heinrich-Heine Universität, Universitätsstraße 1, 40225 Düsseldorf, Germany*
[6]*Department of Physics, Texas A&M University, College Station, Texas 77843, USA*
(Received 30 May 2012; published 19 September 2012)

Harmonic generation in the limit of ultrasteep density gradients is studied experimentally. Observations reveal that, while the efficient generation of high order harmonics from relativistic surfaces requires steep plasma density scale lengths ($L_p/\lambda < 1$), the absolute efficiency of the harmonics declines for the steepest plasma density scale length $L_p \rightarrow 0$, thus demonstrating that near-steplike density gradients can be achieved for interactions using high-contrast high-intensity laser pulses. Absolute photon yields are obtained using a calibrated detection system. The efficiency of harmonics reflected from the laser driven plasma surface via the relativistic oscillating mirror was estimated to be in the range of 10^{-4}–10^{-6} of the laser pulse energy for photon energies ranging from 20–40 eV, with the best results being obtained for an intermediate density scale length.

Ultrashort extreme ultraviolet (XUV) pulses are a promising tool for a wide range of applications including attosecond laser physics and the seeding of free-electron x-ray lasers. Typically, they are created by the nonlinear frequency up-conversion of an intense femtosecond driving laser field in a gaseous medium. Remarkable progress has been made to the present date with efficiencies reaching the level of 10^{-4} at 20 nm wavelengths [1,2]. Such efficiencies are not yet available at shorter wavelengths or for attosecond pulse generation, and the low intensities at which harmonic conversion takes place in gaseous media make harnessing the high peak power in the 0.1–1 PW regime challenging. High-harmonic generation at a sharp plasma-vacuum interface via the relativistically oscillating mirror (ROM) mechanism [3] is predicted to overcome these limitations and to result in attosecond pulses of extreme peak power [4,5].

While other mechanisms such as coherent wake emission can also emit XUV harmonics [6], the ROM mechanism is generally reported to dominate in the limit of highly relativistic intensities, where the normalized vector potential $a_0^2 = I\lambda^2/(1.37 \times 10^{18} \ \mu\text{m}^2 \ \text{W}/\text{cm}^2) \gg 1$. The efficiency of the ROM harmonics is predicted to converge to a power law for ultrarelativistic intensities [7], such that the conversion efficiency is given by $\eta \approx (\omega/\omega_0)^{-8/3}$ up to a threshold frequency $\omega_t \sim \gamma^3$, beyond which the spectrum decays exponentially. Here, γ is the maximum value of the Lorentz factor associated with the reflection point of the ROM process. While these predictions found by Baeva, Gordienko, and Pukhov (BGP) correspond well with the

observations made in experiments using pulse durations of the order of picoseconds in terms of the highest photon energy up to kiloelectronvolts [8,9] and the slope of the harmonic efficiency [10], no absolute efficiency measurements have been reported to date.

The plasma density scale length plays a critical role in determining the response of the plasma to the incident laser radiation. In the picosecond regime, the balance between the laser pressure and the plasma results in the formation of scale lengths and density profiles which are close to ideal for ROM harmonic generation in terms of efficiency for a broad range of laser pulse contrast. Achieving ultrashort (attosecond) XUV pulses requires lasers with few-cycle duration (<10 fs) [11]. Under these conditions, there is insufficient time to modify the density scale length significantly and hence the density gradient and profile become critical control parameters.

Here, we report the first absolute measurements of the ROM harmonic yield. The highest yield is observed for intermediate pulse contrast while the yield declines again for the highest pulse contrast, consistent with a plasma vacuum interface approaching steplike conditions. Achieving and verifying such extreme interaction conditions for relativistic laser intensities is an essential step towards exploiting the potential of a wide range of phenomena, such as bright XUV harmonics, radiation pressure driven ion sources, and the formation of relativistic electron sheets [12].

Two experiments were performed at the 30-fs titanium-sapphire laser systems "Jeti" at the University of Jena and "Arcturus" at the University of Düsseldorf, which

produced similar harmonic spectra. The laser was focused onto targets made of either glass or photoresist at an incidence angle of 45° with a FWHM intensity of $a_0 = 3.5$. At both laser systems the pulse contrast was controlled by a single plasma mirror (PM) with different PM targets. The plasma scale length L_p was calculated using the hydrodynamic simulation code ''Multi-fs'' [13] based on the actual pulse profile measured with a 3rd order autocorrelator. Details are given in Ref. [14]. The highest pulse contrast was achieved with an antireflection (AR) coated PM target and resulted in a scale length of $L_p \lesssim \lambda/10$, while the uncoated borosilicate glass PM target produced an intermediate pulse contrast and $L_p \approx \lambda/5$ [15]. The harmonics' pulse energy was determined using an imaging XUV spectrometer with an 8 mrad × 6 mrad acceptance angle which was calibrated at a synchrotron source [16]. The divergence of the harmonic beam was determined with an angularly resolving XUV spectrometer (see Fig. 1, left side), which allowed the measured yield to be corrected for the observed angular divergence and thus enabled us to obtain the total photon yield. The measurement uncertainty of the photon yield is on the order of 70% (20% spectrometer calibration, 50% uncertainty due to divergence changes). The absolute efficiency $\eta = E_{\mathrm{XUV}}/E_0$ was determined by only considering the fraction of the laser pulse energy E_0 that contributes to the harmonic generation process. Given the strong nonlinearity [17] only the fraction of the laser energy that is focused to sufficiently high intensities ($a_0 \gtrsim 1$) contributes to the interaction. Measurements of the intensity distribution

of the focal spot with a microscope objective showed 20 to 40% of the laser pulse energy to be concentrated within the FWHM of the focus and thus only this fraction is considered when comparing the measured efficiencies to simulations.

Two typical harmonic spectra from photoresist targets are shown in Fig. 1 (right side) using high and intermediate contrast settings, respectively. The angular distribution indicated in Fig. 1 (left side) reveals a divergence of 18.6 mrad for the 21st harmonic using photoresist targets and high contrast. The importance of accounting for the divergence of the harmonic beam when comparing changes in the other parameters is highlighted by the observed changes in divergence under conditions where only the pulse contrast was varied. Changing the pulse contrast from the AR to the glass setting (and hence the scale length from $L_p \approx \lambda/10$ to $L_p \approx \lambda/5$) changes the divergence from 18.6 mrad to 26 mrad for the 21st harmonic. In addition, the divergence of different ROM harmonic orders taken from a single measurement has an almost constant value. This is in excellent agreement with previous observations [18] and fits well with the analysis that the divergence of the ROM harmonic beam is characteristic of a beam with excellent spatial coherence and is determined by the curvature ('dent') of the emission surface imprinted to the target by the light pressure. Since the velocity of the hole-boring process depends on the plasma density [19] the longer scale length deforms more rapidly and should therefore result in a larger divergence in agreement with the observations. This implies that the divergence should be
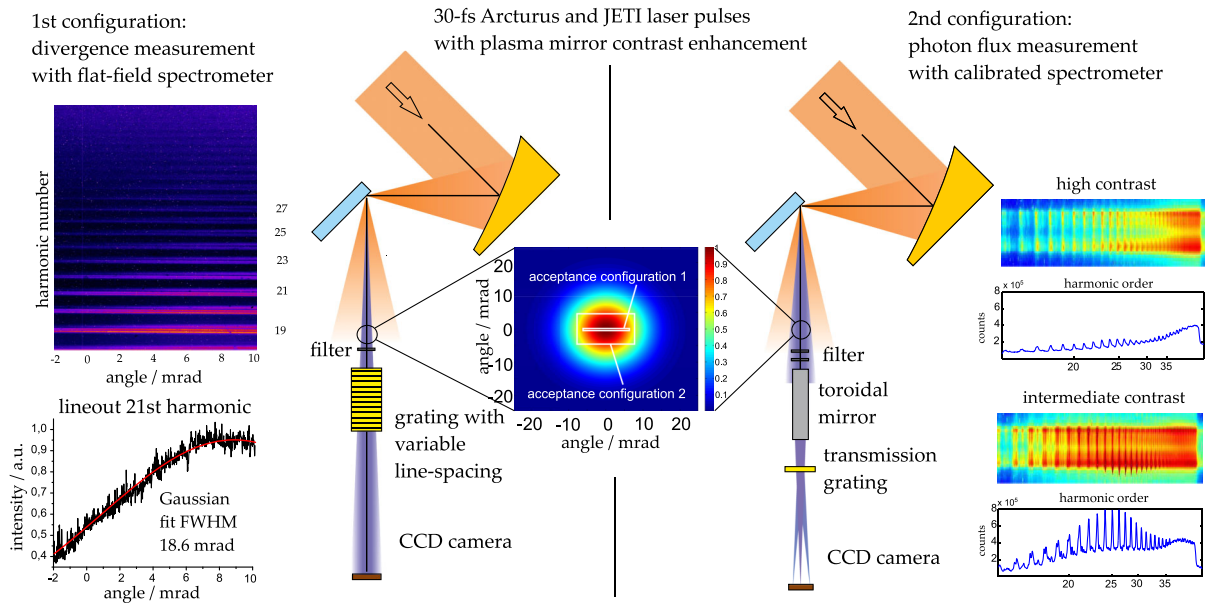

FIG. 1 (color online).   Experimental setup: High-contrast laser pulses were focused with an $f/2$ off-axis parabolic mirror to up to 3×10^{19} W/cm² on a fused silica or plastic coated substrate at 45° *p*-pol. The XUV emission was recorded with two spectrometers separately (in the presented data only plastic coated targets are used). The flat-field spectrometer shown in configuration 1 allows a measurement of the beam divergence. The XUV spectrometer system in configuration 2 has a larger collection angle and was calibrated regarding the incident photon flux. The black line represents the centroid beam of the laser steering into the center of the XUV spectrometers.

reduced substantially in the limit of larger spots or shorter pulses, which would reduce the curvature of the dent at the peak of the pulse respectively.

Until now, it has generally been accepted that achieving sufficiently steep density gradients for the ROM harmonics is the major challenge and hence one would expect the harmonic yield to increase as the prepulse level is reduced. For our conditions and peak intensities, the strongest harmonic emission is observed for intermediate contrast settings (glass PM targets), suggesting that the higher contrast setting with AR PM targets has density scale lengths which are even shorter than the ideal value. The pulse energies E_{XUV} (efficiencies η) for individual harmonics are on the order of 3–24 μJ [(0.1–1) $\times$ 10^{-4}] for the 17th harmonic and approximately 0.3–2.7 μJ [(0.1–1) $\times$ 10^{-5}] for the 21st using different contrast settings. Thus, we find for the first time that we have clear quantitative evidence of ROM generation in the limit of ultrasteep scale lengths. While the benefit of a small, but finite, plasma scale length for the ROM has previously been highlighted by simulations [17,20], the experiments performed so far have required the highest achievable pulse contrast or shortest possible scale length, respectively, in order to optimize the ROM efficiency and beam quality [10,18].

The influence of the plasma scale length has been studied both for glass substrates and photoresist targets that have been coated onto the optically polished glass substrate, reducing the density from 2.2 to $\approx$ 1.1 g/cm^3 (or from $\approx$ 400 to $\approx$ 200n_c in terms of the critical density n_c). The harmonic emission for these high target densities and respective scale lengths is comparable indicating that the enhanced harmonic emission at intermediate scale lengths is not very sensitive for such high peak densities. This means that for our parameters the harmonic emission is enhanced due to the lower density in the plasma gradient and not by using a lower maximum density. Since the reflection point of the ROM is located near the critical density at elongated plasma density ramps, the ROM process is affected by the length of the plasma gradient instead of the maximum plasma density. The observed dependence of the efficiency on the scale length can be understood in terms of the plasma dynamics as follows. First, the denser the plasma and the steeper the gradient, the more the electric field in the skin layer is reduced. Second, the "spring constant" of the electron plasma becomes larger for denser and steeper plasmas, making the ROM harder to drive to the high values of γ associated with a more efficient production of higher harmonic orders.

To make an analytical estimate of the field at the critical density surface we can consider a laser interacting at normal incidence with the target (oblique incidence can be treated by switching into the frame of reference, in which the laser is normally incident [21]). The electrons can gain kinetic energy only through the **E** field of the laser. This field is tangential to the surface and is attenuated due to the skin effect. We assume for the moment, that the
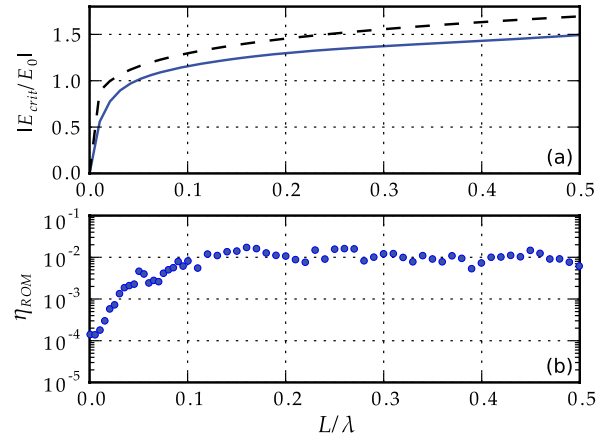

FIG. 2 (color online). (a) Surface field $\mathbf{E}_{\mathrm{crit}}$ at the critical density in units of the incident field $\mathbf{E}_0$, as estimated from the equation in Ref. [22] (black dashed line) and computed exactly by numerical integration for an exponential gradient (blue line). (b) Efficiency of ROM harmonics above the 14th order $\eta_{\mathrm{ROM}} = \int_{14\omega_0}^{\infty} I(\omega) d\omega / P_0$ for $a_0 = 3.5$ at different plasma scale lengths from a set of 1D PIC simulations. Incidence was p-polarized, the plasma ramp is exponential up to a maximum density of $n_e = 200n_c$.

field is nonrelativistic. Evaluating the linear wave equation, we find the threshold condition for it to become relativistic. For a perfectly steep plasma edge, it can be calculated analytically by evaluation of the continuity condition at the plasma edge, yielding $|\mathbf{E}_{\mathrm{crit}}|/|\mathbf{E}_0| = 2\omega_0/\omega_p$. Hence, for our laser and plasma parameters, the field would not be relativistic for a perfect step density profile. This is reflected in Fig. 2(b): in the limit $L \to 0$ there are no relativistic harmonics. The skin field is however enhanced due to a finite density ramp. As a first estimate for finite ramps we may consider the calculation found in Ref. [22], leading to $|\mathbf{E}_{\mathrm{crit}}|/|\mathbf{E}_0| \approx 1.4(\omega_0 L/c)^{1/6}$ at the critical density. This formula becomes exact for linear and extended ($L \gg \lambda$) gradients. For steep exponential ramps, as are expected in the experiments, we find the skin field by numerical integration of the inhomogeneous wave equation. Results of this computation are shown in Fig. 2(a), along with the simple scaling from Ref. [22]. It can be seen that even small scale lengths can considerably boost the skin field compared to the case of steplike profiles. Already at $L = \lambda/20$, there is practically no attenuation at the critical density, but the field can still grow slightly for longer plasma scales. We further note that the simple sixth-root dependence calculated for a linear gradient also yields a reasonable estimate for the exponential gradient, only slightly overestimating the field in comparison to the exact result. Figure 2(b) shows the integrated efficiency η_{ROM} of the ROM harmonics for the same density gradients and a laser amplitude $a_0 = 3.5$. As expected from the previous considerations and Fig. 2(a), it can be seen that the ROM efficiency rises quickly as soon as the skin field

becomes relativistic. For the scale lengths $L > \lambda/10$, the integrated efficiency remains approximately constant at $\eta \approx 7 \times 10^{-3}$ as expected from the ROM model. While the reduction in the critical field explains the drop to very low efficiencies at very short scale lengths, it does not fully explain the efficiency scaling at intermediate scale lengths.

Since the reflection point oscillates around the immobile ion background due to the driving relativistic laser field, another contribution must come from the restoring force due to the quasistatic field generated by the plasma once the electrons are driven out of equilibrium by the laser field. For a given mean displacement of the plasma electrons, the restoring force is proportional to the plasma density. In the limit of a steplike density profile, the restoring force is directly proportional to the maximum plasma density, while in the limit of very long density scale lengths the restoring force is determined by the critical density. In the intermediate case of relevance here, the restoring force will depend in a complex fashion on the density scale length, peak density, and amplitude of the oscillation. While it is not easily possible to express this dependence in a closed analytical form, it is clear that one would expect the effective density and hence the restoring force to be lower for increasingly shallow density gradients resulting in the dependence shown in Fig. 2. Generally, the denser the plasma and the steeper the density ramp, the harder it is for the laser to drive large amplitude oscillations at the plasma surface. This in turn leads to a smaller oscillation amplitude of the ROM and, consequently, to a lower γ factor. An analysis of the electron spring model at ultrarelativistic intensities can be found in Ref. [23]. In agreement with our experimental observations a trend towards higher efficiency for moderately long scale length or low peak densities is expected.

Under our experimental conditions ($a_0 = 3.5$) the efficiencies are still expected to be below the relativistic limit regime where the $\eta \approx (\omega/\omega_0)^{-8/3}$ scaling applies. Figure 3 compares our experimental results to a range of efficiencies predicted by 1D PIC simulations. While the efficiencies are broadly compatible with the range of efficiencies predicted by the simulations, they appear somewhat lower than predictions for the nominal density gradients derived from the measurement of the pulse-contrast and Multi-fs modelling. While, to our knowledge, Multi-fs is the best suited code to calculate the hydro-dynamic expansion under such conditions, the code has not been validated directly by measurements of the scale length under such conditions. Consequently one possible explanation for the discrepancy may be that the density gradients are even steeper than predicted. What is clear both experimentally and from simulations is that the efficiency of the ROM process depends sensitively on the plasma scale length. The generation of surface waves, which have been found in two-dimensional simulations, induce high harmonic emission at angular sidebands [24].
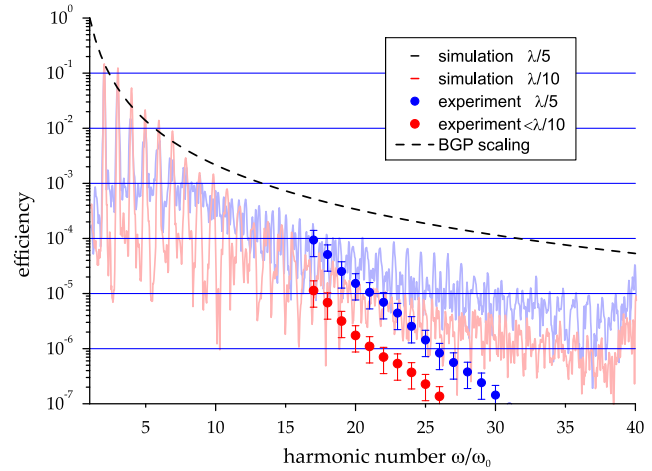

FIG. 3 (color online). Experimental efficiencies (circles) are compared to spectral densities from 1D PIC simulations (lines) for different plasma scale lengths (density $n_e = 200n_c$, exponential density profile). The upper points and graphs (blue) correspond to $L_p = \lambda/5$ and the lower ones (red) to $L_p \leq \lambda/10$. The experimental efficiencies have been normalized to a pulse energy of 250 mJ (energy that is focused to $a_0 > 1$). In the ultrarelativistic limit the efficiencies converge to the BGP power scaling $\eta \approx (\omega/\omega_0)^{-8/3}$ [7].

This may lead to differences between the experimental results and the one-dimensional simulations. Another important effect that is not considered in our simulations is the ion motion. In fact, Thaury and Quéré [17] have shown that the harmonics efficiency in simulations with mobile ions is significantly reduced.

In conclusion, we have investigated harmonic generation in the limit of ultrasteep density gradients and shown the first experimental evidence of the absolute yield reducing for very steep gradients. This demonstrates that relativistic interactions in the limit of ultrasteep density gradients can be achieved by a careful control of the laser parameters. Harmonic efficiency is optimized for intermediate scale lengths. Our results suggest the generation of intense attosecond pulse trains with pulse energies exceeding 10 μJ, thus paving the way towards applications such as nonlinear attosecond experiments or the seeding of free-electron lasers with surface high-harmonic radiation.

[1] I. J. Kim, G. H. Lee, S. B. Park, Y. S. Lee, T. K. Kim, C. H. Nam, T. Mocek, and K. Jakubczak, Appl. Phys. Lett. **92**, 021125 (2008).
[2] G. Sansone, L. Poletto, and M. Nisoli, Nature Photon. **5**, 655 (2011).

[3] P. Gibbon, Phys. Rev. Lett. **76**, 50 (1996).

[4] G. D. Tsakiris, K. Eidmann, J. M.-t. Vehn, and F. Krausz, New J. Phys. **8**, 19 (2006).

[5] S. Gordienko, A. Pukhov, O. Shorokhov, and T. Baeva, Phys. Rev. Lett. **93**, 115002 (2004).

[6] F. Quéré, C. Thaury, P. Monot, S. Dobosz, P. Martin, J.-P. Geindre, and P. Audebert, Phys. Rev. Lett. **96**, 125004 (2006).

[7] T. Baeva, S. Gordienko, and A. Pukhov, Phys. Rev. E **74**, 046404 (2006).

[8] B. Dromey, S. Kar, C. Bellei, D. C. Carroll, R. J. Clarke, J. S. Green, S. Kneip, K. Markey, S. R. Nagel, P. T. Simpson, L. Willingale, P. McKenna, D. Neely, Z. Najmudin, K. Krushelnick, P. A. Norreys, and M. Zepf, Phys. Rev. Lett. **99**, 085001 (2007).

[9] P. A. Norreys, M. Zepf, S. Moustaizis, A. P. Fews, J. Zhang, P. Lee, M. Bakarezos, C. N. Danson, A. Dyson, P. Gibbon, P. Loukakos, D. Neely, F. N. Walsh, J. S. Wark, and A. E. Dangor, Phys. Rev. Lett. **76**, 1832 (1996).

[10] B. Dromey, M. Zepf, A. Gopal, K. Lancaster, M. S. Wei, K. Krushelnick, M. Tatarakis, N. Vakakis, S. Moustaizis, R. Kodama, M. Tampo, C. Stoeckl, R. Clarke, H. Habara, D. Neely, S. Karsch, and P. Norreys, Nature Phys. **2**, 456 (2006).

[11] P. Heissler *et al.*, Phys. Rev. Lett. **108**, 235003 (2012).

[12] V. V. Kulagin, V. A. Cherepenin, M. S. Hur, and H. Suk, Phys. Rev. Lett. **99**, 124801 (2007).

[13] R. Ramis, R. Schmalz, and J. M.-t. Vehn, Comput. Phys. Commun. **49**, 475 (1988).

[14] C. Rödel, M. Heyer, M. Behmke, M. Kübel, O. Jäckel, W. Ziegler, D. Ehrt, M. C. Kaluza, and G. G. Paulus, Appl. Phys. B **103**, 295 (2011).

[15] M. Behmke, D. an der Brügge, C. Rödel, M. Cerchez, D. Hemmers, M. Heyer, O. Jäckel, M. Kübel, G. G. Paulus, G. Pretzler, A. Pukhov, M. Toncian, T. Toncian, and O. Willi, Phys. Rev. Lett. **106**, 185002 (2011).

[16] S. Fuchs, C. Rödel, M. Krebs, S. Hädrich, A. E. Paz, S. Kuschel, J. Bierbach, M. Wünsche, V. Hilbert, U. Zastrau, E. Förster, J. Limpert, and G. G. Paulus (to be published).

[17] C. Thaury and F. Quéré, J. Phys. B **43**, 213001 (2010).

[18] B. Dromey, D. Adams, R. Hörlein, Y. Nomura, S. Rykovanov, D. Carroll, P. Foster, S. Kar, K. Markey, P. McKenna, D. Neely, M. Geissler, G. Tsakiris, and M. Zepf, Nature Phys. **5**, 146 (2009).

[19] S. C. Wilks, W. L. Kruer, M. Tabak, and A. B. Langdon, Phys. Rev. Lett. **69**, 1383 (1992).

[20] A. Tarasevitch, K. Lobov, C. Wünsche, and D. von der Linde, Phys. Rev. Lett. **98**, 103902 (2007).

[21] A. Bourdier, Phys. Fluids **26**, 1804 (1983).

[22] W. Kruer, *The Physics of Laser Plasma Interactions*, (Westview Press, Boulder, 2003).

[23] A. A. Gonoskov, A. V. Korzhimanov, A. V. Kim, M. Marklund, and A. M. Sergeev, Phys. Rev. E **84**, 046403 (2011).

[24] D. an der Brügge, N. Kumar, A. Pukhov, and C. Rödel, Phys. Rev. Lett. **108**, 125002 (2012).